STUDY ON NUMERICAL SIMULATION OF FLOW STRUCTURES IN A CURVED OPEN CHANNEL

FIKRY PURWA LUGINA
Hiroshima University, Hiroshima, Japan, m183691@hiroshima-u.ac.jp

TATSUHIKO UCHIDA
Hiroshima University, Hiroshima, Japan, utida@hiroshima-u.ac.jp

YOSHIHISA KAWAHARA
Hiroshima University, Hiroshima, Japan, kawahr@hiroshima-u.ac.jp

ABSTRACT

Understanding flow characteristics in an open channel is crucial to assess velocity distribution and sediment transport patterns for bank protection. Numerical models are widely used to clarify the complex phenomena of flow structures and sediment transport in rivers after validation with reliable experimental datasets. However, the applications of a detailed three-dimensional (3D) model are still limited to small-scale phenomena, such as local scouring in an experimental channel because of long computational time, large memory requirements, and numerous computational tasks. Numerous depth-integrated models have been proposed to solve these problems. Numerical calculation validation was performed in this study by comparing a set of numerical models with a laboratory experiment conducted by De Vriend (1979). Numerical calculation method applied in this research is the bottom velocity computation (BVC) method, which evaluates bottom velocity distributions without computing the vertical distribution of velocity and pressure intensity, based on a depth-integrated method with horizontal vorticity equations. This paper presents the applicable ranges of a two-dimensional (2D) model and a quasi 3D model of a simplified bottom velocity computation (SBVC) model with shallow water assumption. A modified discretization for the dispersion term using the upwind scheme approach is introduced, and its merits over the previous scheme. The advantages of employing the SBVC method are demonstrated through a comparison with the 2D model. Measurement results indicate that the SBVC method can reproduce flow structures in a curved open channel.

Keywords: Open channel, depth-integrated model, curved channel,

1. INTRODUCTION

Understanding flow characteristics in an open channel is crucial to assess velocity distribution and sediment transport patterns for bank protection. Numerical methods are widely used in modeling river hydrodynamics because of their cost effectiveness over experiments and field measurements. They are effective in clarifying the complex phenomena of flow structures and sediment transport after validation with reliable experimental datasets (Wormleaton, 2010). Understanding the mechanism of flow structures is useful for river engineers.

Two-dimensional (2D) numerical methods have been used to simulate flows and temporal variations in bed topographies during floods. However, 2D numerical methods present limitations when defining complex phenomena, such as three-dimensional (3D) flows. Lane et al. (1999) compared the capabilities of 2D and 3D model approaches in calculating the flow process and sediment transport; their results showed that the 3D model demonstrated a higher predictive ability. Researchers have studied 3D models (Shukla and Shiono (2008); Morvan, et. al. (2002); Jing et. al. (2008)) and reported that they demonstrated good ability in simulating flow structures in meandering channels. However, the applications of 3D models are still limited to small-scale phenomena, such as local scouring in experimental channels because of their long computational time, large memory requirements, and numerous computational tasks.

A number of depth-integrated models have been proposed to solve this problem. Uchida and Fukuoka (2016) developed a depth-integrated model, known as bottom velocity computation (BVC). The BVC method is an integrated multiscale simulation of flows and bed variations in rivers, which can evaluate vertical distributions of horizontal and bottom velocities by introducing depth-averaged horizontal vorticity and horizontal

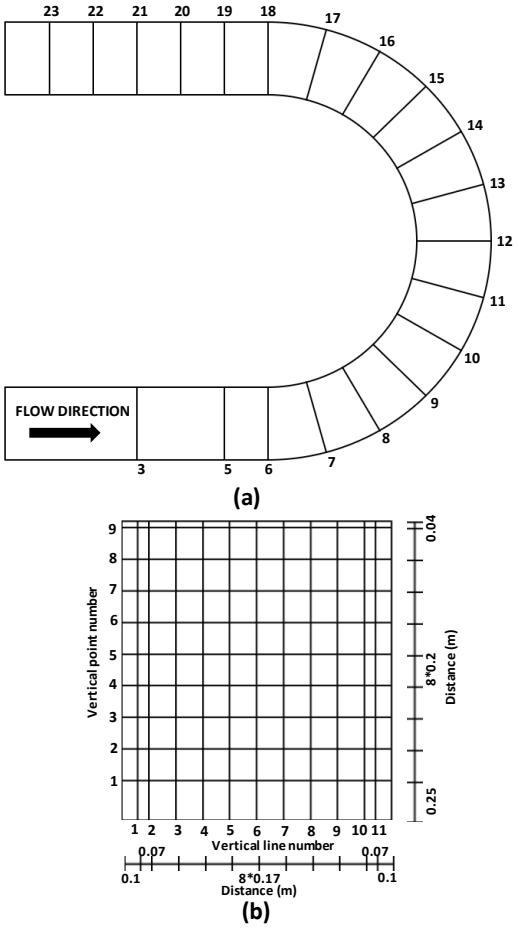

Figure 1. De Vriend (1979) experiment (a) curved open channel (b) messes of velocity measuring point

momentum equations on a water surface to shallow water equations. The BVC method with shallow water assumption is known as simplified bottom velocity computation (SBVC). The objective of this study is to analyze the ability of the BVC method in calculating flow structures in a curved open channel by comparing it with experimental data.

2. METHODS

2.1 Experimental conditions

The configuration of the physical model of the experiment conducted by De Vriend (1979) is shown in Fig. 1. Measured data of water surface elevation and velocity along the channel at the cross sections are available. The experiment conditions for the simulated flow are presented in Table. 1.

The velocity data were measured in 21 cross-sections, including 13 sections in the curved part of the channel, which were equally spaced at 15° intervals from 0° to 180°. Six more sections in the downstream straight channel at 1 m intervals and two other sections were measured in the upstream straight segment; one was 1 m and the other was 4 m upstream of the first curved channel section. At each cross section, measurements were performed along 11 vertical lines; furthermore, each vertical line comprised nine measuring points.

Table 1. Experiment condition for flow measurement.

Bed slope *So*	Discharge Q (m^3/s)	Depth (m)	Width (m)	Channel length (m)	Inner radius r (m)	Outer radius R (m)
0.0	0.18	0.189	1.7	23.35	3.4	5.1

2.2 Numerical model

The BVC method was developed based on Eq. (3), which was derived by depth-integrating the horizontal vorticity with the shallow water assumption, in which the ratio of the representative water depth h_0 to representative horizontal scale L_0 is small, i.e., $\varepsilon_S = \frac{h_0}{L_0} \approx \frac{W_0}{U_0} << 1$ (ε_s: shallowness parameter).

$$u_{bi} = u_{si} - \varepsilon_{ij}\Omega_j h, \tag{1}$$

where u_{bi}: bottom velocity, u_{si}: water surface velocity, Ω_j: depth-averaged vorticity, h: water depth, w_s, w_b: vertical velocity on water surface and bottom, respectively, z_s: water surface level, and z_b: bottom level. The bottom velocity was evaluated by the water surface velocity and depth-averaged vorticity. To evaluate the bottom velocity shown in Eq. (1), the governing equations of the BVC method were composed of the depth-integrated horizontal vorticity (Eq. (2)) and water surface velocity (Eq. (3)), in addition to the depth-integrated continuity equation (Eq. (4)) and depth-integrated horizontal momentum equation (Eq. (5)).

$$\frac{\partial \Omega_i h}{\partial t} = ER_{\sigma i} + P_{\omega i} + \frac{\partial hD_{\omega ij}}{\partial x_j}, \tag{2}$$

where $\Omega_i$is the depth-averaged horizontal vorticity in the i direction, $ER_{\sigma i}$ the rotation term of the vertical vorticity, $P_{\omega i}$ the production term of vorticity from the bottom vortex layer, and $D_{\omega ij}$ the horizontal vorticity flux due to convection, rotation, dispersion, and turbulence diffusion.

$$\frac{\partial u_{si}}{\partial t} + u_{sj}\frac{\partial u_{si}}{\partial x_j} = -g\frac{\partial z_s}{\partial x_i} + P_{si}, \tag{3}$$

where g denotes gravity, and $P_{si}$the production term due to the shear stress acting on the thin water surface layer δz_s.

$$\frac{\partial h}{\partial t} + \frac{\partial U_i h}{\partial x_i} = 0 \tag{4}$$

$$\frac{\partial U_i h}{\partial t} + \frac{\partial U_i U_j h}{\partial x_j} = -gh\frac{\partial z_s}{\partial x_i} - \frac{\tau_{bi}}{\rho} + \frac{\partial hT_{ij}}{\rho \partial x_j}, \tag{5}$$

where U_i is the depth-averaged horizontal velocity in the i direction, τ_{bi} the bed shear stress, and T_{ij} the horizontal shear stress due to turbulence and vertical velocity distribution. The vertical distributions of the horizontal velocities are expressed by the cubic function (Eq. (6)) using the depth-averaged velocity U_i, velocity differences δu_i , Δu_{ij}, and dimensionless depth η.

$$u_i = \Delta u_i\left(12\eta^3 - 12\eta^2 + 1\right) + \delta u_i\left(-4\eta^3 + 3\eta^2\right) + U_i, \tag{6}$$

where, Δu_i: $u_{si} - U_i$, δu_i: $u_{si} - u_{bi}$, η: $(z_s - z_b)/h$.

In this study, two numerical calculations were compared with the experiment by De Vriend (1979), as well as the 2D and SBVC models.

2.3 Evaluation method of the dispersion term

The effect of the dispersion term in a curved channel has been observed by Lien et al. (1999); they discovered that the dispersion term was an important term for describing secondary flow effects in curved-flow simulations. Dispersion changed abruptly near the entrance and exit of the bend, which was attributed to the transverse convection of the momentum.

In numerical model, conservation of some quantities such as momentum transfer is a basic property and it is important that the discretization scheme preserves the same feature. The discretization scheme caused some numerical oscillations since it loses most of the stability properties of the continuous problem. Many numerical methods were applied for these problems, such as the finite difference method (FDM), finite element method (FEM), and finite volume method (FVM). The finite volume methods (FVM) have been widely used as effective discretization techniques for partial differential equations (Hermeline, 2000; Manzini and Russo, 2008). The FVM method combining with upwind scheme has overcome the numerical oscillation (Liang and Zhao, 1997).

In the present method, one of the upwind schemes (CIP-CSL) was applied, whereas a centered scheme was applied in the dispersion term. The last term in Eq. (5) is the horizontal momentum transfer, which comprises a shear stress term due to molecular and turbulent motions and a dispersion term with vertical velocity distribution.

$$T_{ij} = \tau_{ij} + \overline{u_i' u_j'}, \tag{7}$$

where $u_i' = u_i - U_i$. The dispersion term in Eq. (7) and the convection term in Eq. (5) are from the same convection term of the Reynolds-averaged Navier–Stokes equation before the depth-averaged integration.

A discretization method with the dispersion term in Eq. (7) is proposed herein. Applying the first-order upwind scheme to momentum transfer $u_i u_j$, the dispersion term D_{ij} is derived as follows:

$$D_{ij} = \varepsilon \frac{\partial U_i}{\partial x_j} \qquad \varepsilon = \begin{cases} \dfrac{\left|\delta u_j\right| - \left|2U_j\right|}{8} \Delta x_j, & \left|\delta u_j\right| > \left|2U_j\right| \\ 0, & \left|\delta u_j\right| < \left|2U_j\right| \end{cases} \tag{8}$$

Eq. (8) was added to evaluate the dispersion term of the last term in Eq. (7) for the momentum equation in the *i* direction.

3. RESULTS AND DISCUSSION

Fig. 2 shows a comparison of the water surface profile. Fig. 2(a) shows the result obtained by the experiment. The water surface profile was uniform in the section located before the curved part. Once the flow entered the curved part, the water level increased at the outer bank and decreased at the inner bank. The consideration of the secondary flow effect can decrease the slope of the super-elevation between the inner and outer banks. When the flow passed the curved part, the water surface profile became deeper at the outer wall and exhibited a skewed pattern.

The results of the numerical calculations were validated against the experiment of de Vriend (1979). Figs. 2(b) and 2(c) show the results of the 2D and SBVC models, respectively; as shown, both models can reproduce the

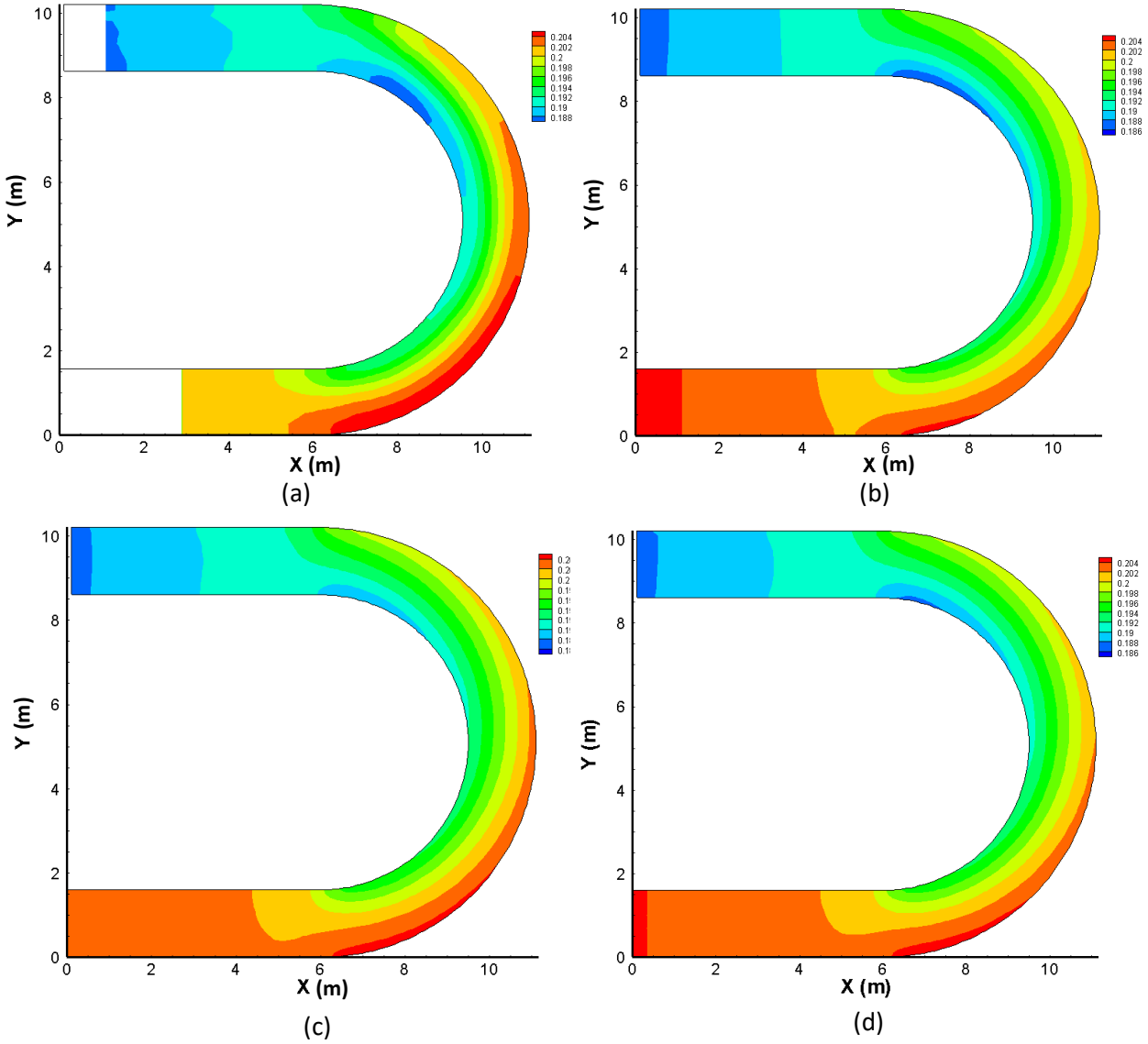

Figure 2. Water surface profile along the streamwise direction. (a) De Vriend (1979), (b) 2D, (c) SBVC, (d) SBVC_updated

water surface profile from the experiment. The 2D model has a uniform water surface profile after leaving the curved part, and it cannot reproduce the skewed pattern after leaving the curved part. Meanwhile, the SBVC model can reproduce the skewed pattern after leaving the curved part; however, it cannot reproduce the lower depth of the water surface profile around the inner curved part.

Fig. 2(d) shows the water surface profile of an updated SBVC. As shown, the treatment reproduced the water surface profile from the experiment satisfactorily. Along the inner curved part, it can reproduce the lower depth pattern. After leaving the curved part, it exhibits a skewed pattern, consistent with the experiment.

Fig. 3 shows a comparison of the depth-averaged velocity along the streamwise direction. The behavior of secondary flows in a curved channel has been discussed by de Vriend (1979); before entering the curved part, the velocity exhibited a uniform pattern. Once the velocity entered the curved part, the velocity near the inner bank decreased gradually, whereas the velocity near the outer bank increased. After leaving the curved part, the outer bank became dominant owing to the large intensity of the secondary flow, which was the transverse convection of momentum transfer.

Fig. 3(a) shows a comparison between the de Vriend (1979) and 2D models. The depth-averaged velocity pattern became uniform after leaving the curved part. This shows that apart from being unable to describe complex phenomena, the 2D model cannot produce the secondary flow effect in a depth-averaged velocity distribution. Fig. 3(b) shows the comparison between the de Vriend (1979) and SBVC models before adding the diffusion term. The calculation yielded a higher velocity along the outer wall than the experimental one; this was caused by the oscillation from the dispersion term. Meanwhile, SBVC_updated reproduced a depth-averaged velocity distribution that was similar to the experimental one, as shown in Fig. 3(c).

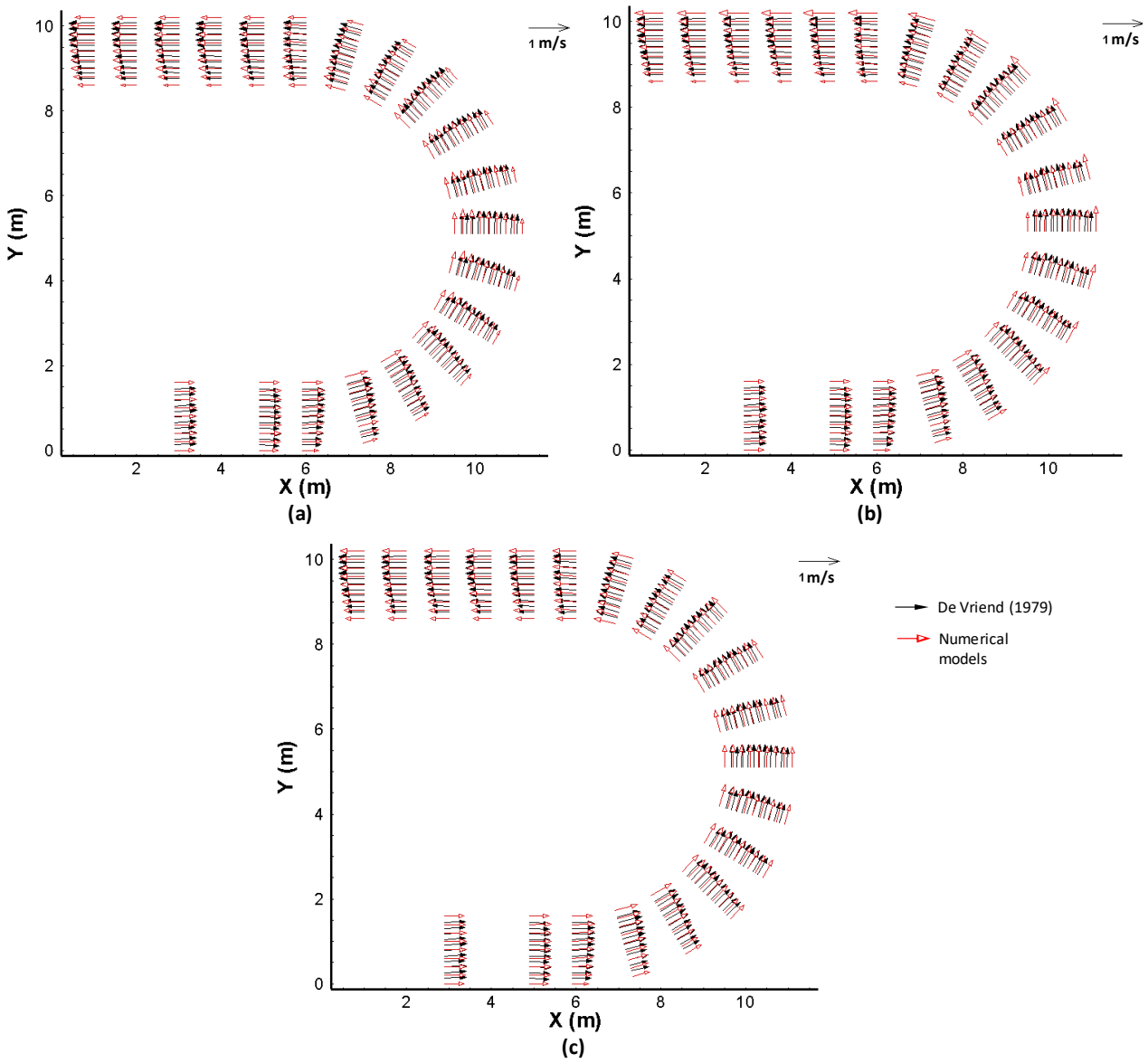

Figure 3. Depth average velocity distribution along the streamwise direction. (a) De Vriend (1979) and 2D, (b) De Vriend (1979) and SBVC, (c) De Vriend (1979) and SBVC_updated

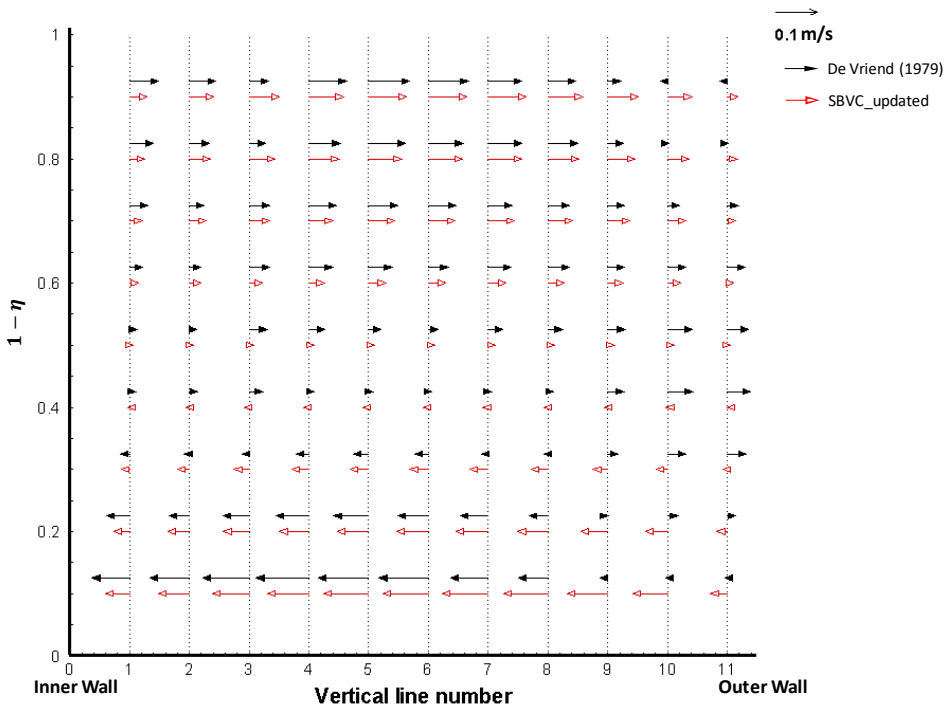

Figure 4. Comparison of secondary flow structures at cross-section 12.

Fig. 4 shows a comparison of secondary flow structures at cross section number 12. The SBVC method could reproduce secondary flow structures; the major secondary flow moved outward from the wall (moved from the inner wall to the outer wall). At the surface, the flow moved to the outer wall; at the bottom, the flow moved to the inner wall. However, the SBVC model could not reproduce velocity structures at the upper-outer and bottom-outer walls. The experimental data indicated that the flow moved anticlockwise. In the SBVC model, the flow moved outward, which was one of the limitations of the SBVC model.

4. CONCLUSION

In general, the proposed model demonstrated satisfactory performance compared with the experimental data. Both the 2D and SBVC models produced a water surface profile and a depth-averaged velocity distribution. Meanwhile, only the SBVC model could describe secondary flow structures. A modified discretization for the dispersion term using the upwind scheme approach was introduced, and its merits over the previous scheme were presented. The results indicated that the scheme produced less numerical diffusion and dispersion than the centered scheme.

REFERENCES

De Vriend, D. J. (1979). Flow measurements in a Curved Rectangular Channel, Internal Report, No. 9-79.

Hermeline, F. (2000). A finite volume method for the approximation of diffusion operators on distorted meshes. *Journal of Computational Physics*, 160:481-499.

Jing, H., Guo, Y., Li, C., and Zhang J. (2009). Three-dimensional numerical simulation of compound meandering open channel flow by the Reynolds stress model. *International Journal for Numerical Methods in Fluids*, 59:927-943.

Lane, S. N., Bradbrook, K. F., Richards, K. S., Biron, P. A., and Roy, A. G. (1999). The application of computational fluid dynamics to natural river channels: three-dimensional versus two-dimensional approaches. *Geomorphology*, 29:1-20.

Liang, D. and Zhao, W. (1997). A high-order upwind method for the convection-diffusion problem. *Computer Methods in Applied Mechanics and Engineering*, 147:105-115

Lien, H. C., Hsieh, T. Y., Yang, J. C., and Yeh K. C. (1999). Bend-flow simulation using 2D depth-averaged model. *Journal of Hydraulic Engineering*, 125:1097-1108.

Manzini, G., Russo, A. (2008). A finite volume method for advection-diffusion problems in convection-dominated regimes. *Computer Methods in Applied Mechanics and Engineering*, 197:1242-1261.

Morvan, H., Pender, G., Wright, N.G., and Ervine, D. A. (2002). Three-dimensional hydrodynamics of meandering compound channels. *Journal of Hydraulic Engineering*, 128(7):674-782.

Petrie, J. and Diplas, P. (2016). Evaluation of the logarithmic law of the wall for river flows. *River Research and Applications*, 32:1082-1093.

Shukla, D. R. and Shiono, K. (2008). CFD modelling of meandering channel during floods. *Proceedings of the Institution of Civil Engineers Water Management*, 161(1):1-12.

Uchida, T. and Fukuoka, S. (2016). Nonhydrostatic uasi-3D model coupled with dynamic rough wall law for simulating flow over a rough bed with submerged boulders. *Journal of Hydraulic Engineering,* 142(11):04016054.

Wormleaton, P.R. and Ewunetu, M. (2006). Three-dimensional k–∈ numerical modelling of overbank flow in a mobile bed meandering channel with floodplains of different depth roughness and planform. *Journal of Hydraulic Research,* 44(1):18-32.